Model Nanocomposites Based on Laponite and Poly(ethylene oxide): Preparation and Rheology

Anthony Loiseau and Jean-François Tassin*

Polymères, Colloïdes, Interfaces, UMR CNRS 6120, Université du Maine, 72085 Le Mans Cedex 9, France

Received June 14, 2006; Revised Manuscript Received October 3, 2006

ABSTRACT: This paper describes the preparation of model nanocomposites based on geometrically well-defined particles (laponite) dispersed into a PEO matrix of narrow molecular weight distribution. The preparation involves the protection of the laponite particles with an adsorbed or a grafted layer of PEO chains. The adsorption is carried out in solution and the particles are recovered with a freeze-drying process. The surface coverage can be controlled from this process to obtain either starved or saturated particles. The protected particles are dispersed into the PEO matrix in the molten state thanks to a microcompounder. The linear viscoelastic properties are studied in the molten state and analyzed in light of the state of dispersion of the particles as determined by X-ray diffraction. The dispersion of the particles as individual entities is shown to increase with the surface coverage of the particles and grafted chains appear more efficient than adsorbed ones to achieve exfoliation. The formation of a gel is obtained above a critical volume fraction (on the order of 0.2−0.4% depending on the protection of the particles) where the elastic moduli increase with a power law of the frequency. The elastic modulus and the yield stress in the gel state increase with a power law of the particle's concentration with exponent 4.5 and 3.3 respectively, in agreement with a fractal arrangement of the particle's network in the matrix.

Introduction

The field of polymer nanocomposites, especially involving layered clay silicates as fillers, has attracted an increasing number of researches throughout the last years. Dispersion of a few percent of nanoscale clay platelets can lead to improved polymer properties, especially mechanical, thermal, and barrier properties.[1,2] These materials can be considered as suspensions of highly anisotropic particles, with various kinds of dispersions states, showing interesting, but not yet fully understood, rheological behavior when the polymer matrix is in the molten state.

Several methods were described to obtain polymer layered silicate nanocomposites (PLSN) in a large variety of polymer matrixes:[1] in situ intercalative polymerization, swelling followed by dispersion in solution and melt intercalation where the particles are mixed with the polymer in the molten state. Vaia et al.[3] showed that melt intercalation is an attractive approach, since it can be easily carried out using conventional polymer processing equipments like twin-screw extruders.

Different limiting typical states of dispersion have been described:[4] a *demixed macrocomposite*, in which the particles are gathered into large entities with a typical size on the order of several micrometers, an *intercalated* structure in which polymer chains might be inserted into the galleries between the clay platelets which remain still ordered in a multilayered structure, and an *exfoliated* (or delaminated) *structure* where the silicate particles are separated and randomly dispersed in a continuous polymer matrix. In many practical situations the dispersion state appears to be a mixture of intercalated and exfoliated particles. To improve the dispersion as individual particles, specific interactions between the particles and the polymer matrix have to be introduced. In most of the cases, the inorganic cations at the surface of the clay particles are exchanged by long tail alkylammonium groups in order to bring them an organophilic character and improve the compatibility with the polymer matrix. Furthermore, when dispersion into a nonpolar matrix such as polyethylene or polypropylene is carried out, a statistical copolymer based on the matrix and containing polar entities such as maleic anhydride is often added as a compatibilizing agent.[5,6]

The rheological behavior is highly dependent on the detailed structure of the materials and rheology appears as a complementary technique with regard to X-ray diffraction and transmission electron microscopy to characterize, at least qualitatively, the state of dispersion.[7−9] A general rheological trend for nanocomposite materials in the linear viscoelastic regime is the appearance of a transition from a liquidlike behavior (characterized by a finite zero shear viscosity) to a pseudo solidlike behavior with a divergence of the viscosity at low shear rates and the apparition of a plateau of the storage modulus at low frequency, which is higher than the loss modulus.[4] The increase in particles concentration is driving this transition, although no universal value of the critical concentration can be obtained. This transition has been attributed to the existence of a three-dimensional percolated network.[10−15] This behavior also appears in suspensions of other types of particles. Recent studies with nanocomposites based on carbon nanofibers agree with the existence of a critical gel for a given concentration,[16] for which the dynamic moduli follow the same power law with frequency, according to the Winter−Chambon criterion.[17,18] With other types of aggregating particles, Zhang et al.[19] report on a critical volume fraction of 2% of silica nanospheres in molten poly(ethylene oxide), much below the percolation transition of spheres.

Large amplitude oscillations or continuous shearing eliminate the solidlike behavior of PLSN.[10] This observation was explained by a breakdown of the particles network and the particle's orientation under shear.[11]

However, to our best knowledge, although converging behaviors of nanocomposite materials in the molten state exist, and although the sensitivity of dynamic moduli to the state of

* To whom correspondence should be addressed.

10.1021/ma061324w CCC: $33.50
Published on Web 11/30/2006

dispersion is often reported, quantitative data are lacking for critical concentrations and scaling relationships between the elastic modulus and the particles concentrations in the case of platelike particles.

To go further in this direction a study of model nanocomposites has been carried out. The model character relies on the choice of both the polymer and the particles, as well as on the compatibilization between the polymer and the particles. A polymer, available in a large variety of molecular weights and with narrow distribution of molecular weights, has been considered. With this respect, taking into account the need of an hydrophilic polymer, as it will be explained below, poly(ethylene oxide) (PEO) was chosen. Furthermore, instead of using montmorillonite-derived particles, which do not show a well-defined shape and can exhibit a large variety of lateral dimensions, which can eventually be affected by the blending process,[20] we decided to use synthetic clay particles, namely laponite, that possess a better defined shape with a rather low polydispersity and lower lateral dimensions than montmorillonite.[21,22] Laponite particles bearing a protecting layer of PEO have been used, to bring compatibilization between the particles and the matrix.

Poly(ethylene oxide) (PEO)/clay nanocomposites have been considered and studied for their applications as polymer electrolytes.[23−26] PEO chains have a high affinity for the clay particles due to their interactions with cations[25] and have been found to be able to intercalate into the interlayer of montmorillonite as shown by an increase of the basal spacing.[9,24,27−29] The same result was found with laponite clay.[30,31] Although several studies have dealt with the rheological behavior of laponite dispersed in PEO solutions (usually of high molecular weight),[32−37] we are not aware of any study dealing with the rheological behavior in the molten state of laponite/PEO nanocomposite.

Laponite is a synthetic clay that has been used as a model for clay suspensions. The disklike shape particle has a diameter of about 25−30 nm and a thickness of 1 nm.[21,22,38] When dispersed in water, laponite particles shows highly negatively charged faces and some positive charges on their edges. Laponite particles can be well dispersed in deionized water at pH = 10.[22,39] However, attractive electrostatic interactions progressively lead to the formation of a gel by an aggregation process with kinetics that are strongly dependent on concentration and ionic strength.[40,41] It has also been shown that PEO chains adsorb on laponite particles, leading to a reduction of the gelation rate thanks to an additional steric stabilization through the absorbed chains[42,43] and that micrometer scale network like structures can be formed in water with high molecular weight PEO.[34] Taking advantage of negative charges onto the particles, PEO chains containing a quaternary ammonium salt on one end (instead of the classical hydroxyl group) can develop strong electrostatic interactions with the clay platelets, leading in solution to grafted chains rather than statistically adsorbed ones, with an higher surface coverage as shown by Mongondry et al.[44]

This system is very versatile since the molecular characteristics of the protecting chains as well as those of the matrix can be varied independently. In the present study, rheological properties of nanocomposites will be discussed in relation to the dispersion state induced by the preparation process and concentration of particles.

Experimental Section

Materials and Preparation. Poly(ethylene oxide) of weight-average molecular weight M_w = 10000 g/mol was purchased from Fluka and was used as received. The melting temperature as measured by DSC is 68.4 °C, while size exclusion chromatography (SEC) in THF gave M_w = 9850 g/mol and M_w/M_n = 1.08.

To compare the influence of adsorbed vs grafted chains a PEO of 2000 g/mol containing an hydroxyl group at one end (Aldrich) was functionalized as described by Mongondry et al.[44] in order to obtain a trimethylammonium terminated PEO chain.

Laponite RD, obtained form Rockwood additives Ltd. (U.K.), with density 2570 kg/m^3 was used. The cation exchange capacity is 0,95 mequiv/g, and the specific surface is 750 m^2/g.

Samples were prepared in two steps. The laponite powder and PEO were dispersed separately under gentle stirring for 24 h in Milli-Q water set at pH 10 (using NaOH in order to avoid clay degradation). The two solutions were mixed with different proportions in order to control the amount of PEO adsorbed onto the particles, and were kept under agitation for 24 h. The PEO chains adsorb or graft onto the surface of the particles, depending whether simple PEO or quaternized chains are involved. The adsorption isotherms of PEO chains onto laponite have been studied in a previous work. The surface coverage at saturation is of 1.14 g/g with PEO 10000,[42] 0.43 g/g with PEO 2000, and 1.09 g/g with Me_3N^+PEO 2000.[44] By using different proportions of PEO solutions with respect to laponite dispersion, different ratios polymer/particles allowed us to obtain *bare or unprotected particles*, *starved particles* (1/1 laponite and PEO by weight), and *saturated particles* (1/2.5 laponite and PEO by weight). A freeze-drying procedure was used to keep as much as possible the state of dispersion and to recover the protected particles, as a fluffy powder. This powder is called hereafter a "masterbatch" since it contains a high concentration of particles bearing adsorbed or grafted polymer chains and eventually free chains (especially in the case of the saturated particles).

In a second step, the particles were incorporated into the polymer matrix PEO 10000, in the molten state, using a Haake Minilab microcompounder under corotating twin-screws operating at 80°C, 200 rpm for 10mn.

The particles concentration in the materials will be hereafter defined by the amount of bare laponite. Eventually adsorbed or grafted PEO chains are thus not included in the particle's concentration.

Characterization. X-ray Diffraction (XRD). The extent of dispersion of laponite particles as individual particles was qualitatively determined by detecting the position and the intensity of the first-order Bragg peak into the X-ray diffraction spectrum. The X-ray experiments were performed using a Philips X-Pert apparatus in the reflection mode, with Cu Kα radiation, λ = 1541 Å. The generator was operated at a voltage of 40 kV with a current of 30 mA. To compare the relative intensity of the Bragg peak around 0.37 Å^{-1}, and avoid the effect of small variations in experimental parameters, the data were corrected for baseline, PEO content and PEO crystallinity. The baseline in the range 0.75−0.8 Å^{-1} which reflects essentially the polymer contribution (electron density) was subtracted. The intensity was further normalized using the PEO peak at 1.35 Å^{-1} which reflects the crystalline fraction of the polymer, and thus the polymer concentration and the crystallinity. The polymer crystallinity was measured by DSC as described below.

Differential Scanning Calorimetry (DSC). DSC analysis was carried out on a 2920 modulated DSC from TA Instruments in sealed aluminum pans. Calibration was checked and adjusted from the melting endotherm of an indium standard.

The samples were heated at 120 °C, annealed in the molten state for 3 min and cooled at 5 °C/min until −20 °C. Heating rate of 10 °C/min was applied, and peak melting temperature and degree of crystallinity (χ_c) were measured. The enthalpy of fusion of PEO was taken as 197.8 J/g.[57] Since crystallinity is only relevant for the PEO chains, all the data were corrected by the weight fraction of PEO (including both laponite protecting chains and matrix chains). The polymer crystallinity changed from 91% for pure PEO down to 80% for nanocomposites containing 10 wt % particles. The crystallinity data were used to normalize the X-ray measurements and eliminate experimental factors like beam intensity.

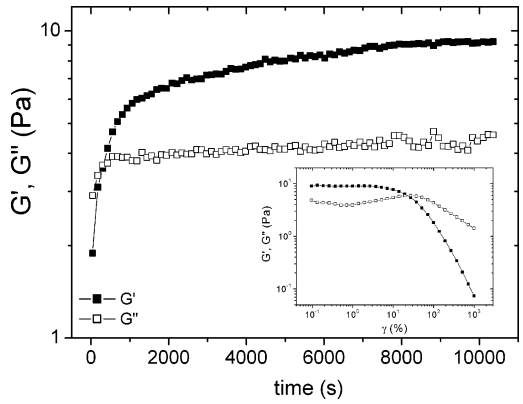

Figure 1. Increase of the moduli with time during thermal equilibration. The inset shows the dynamic moduli vs the applied shear (determination of the linear domain). (Starved laponite particles are at 6.5 wt % in PEO 10000.)

Rheological Measurements. Oscillatory-shear measurements of nanocomposites were performed on a stress controlled rheometer (RS100 manufactured by Haake). All rheological data were taken at 80°C in parallel plate geometry (60 mm diameter, gap ≈ 1 mm). Such geometry ensures that the gap is much larger than the size of possible aggregates. Oscillatory shear measurements were performed in the linear domain in the so-called stress controlled mode, leading to deformations that are below 1%. Interestingly, the linear domain was found to be restricted to lower deformations at low frequencies rather than at higher ones. The rheological data were collected after mechanical equilibration of the sample on the rheometer. Indeed, after thermal equilibration an increase of the moduli with time is observed. Equilibration times were on the order of 5 h. This effect is illustrated in Figure 1, which also shows the very limited linear domain in the inset.

After the dynamic measurements, flow properties of the nanocomposites were characterized in the so-called steady-state flow mode by stepwise increase of the applied stress and further creep during 5 min at the end of which the resulting shear rate is collected.

Results

Influence of Laponite Concentration. Figure 2a shows the X-ray diagrams for various concentrations of starved particles blended into the PEO matrix. The curves were corrected as described in the Experimental Section. X-ray data clearly show that the particles are not dispersed as individual particles, but that stacks of three to four particles (as estimated from the width of the Bragg peak) also exist. This number does not seem to depend on the concentration. However the Bragg peaks at 0.331 $Å^{-1}$ showed an increase of the *d* spacing from 12 Å for neat freeze-dried laponite to 18.9 Å. Some PEO chains are thus intercalated between the particles, as already observed by Loyens et al.[30,45] for melt prepared samples as well as Doeff et al.[23] for concentrated samples prepared from solution. The height of the Bragg peak, normalized by the concentration of particles decreases when the concentration increases. This shows that the relative quantity of PEO intercalated particles is changing. The particles that do not appear in this Bragg peak either exist as compact aggregates of laponite particles without short range order (virgin laponite powder does not show any peak), as PEO intercalated particles with a long range order distance higher than 4 nm or as exfoliated particles.

A small angle X-ray scattering spectrum acquired on the 6.5 wt % shows that no correlation peak associated with a long distance range can be evidenced (Figure 2b).

Figures 3a and 3b respectively show the frequency dependence of the dynamic moduli G' and G'' for various concentrations of laponite ranging from 0 to 10 wt %. In these figures

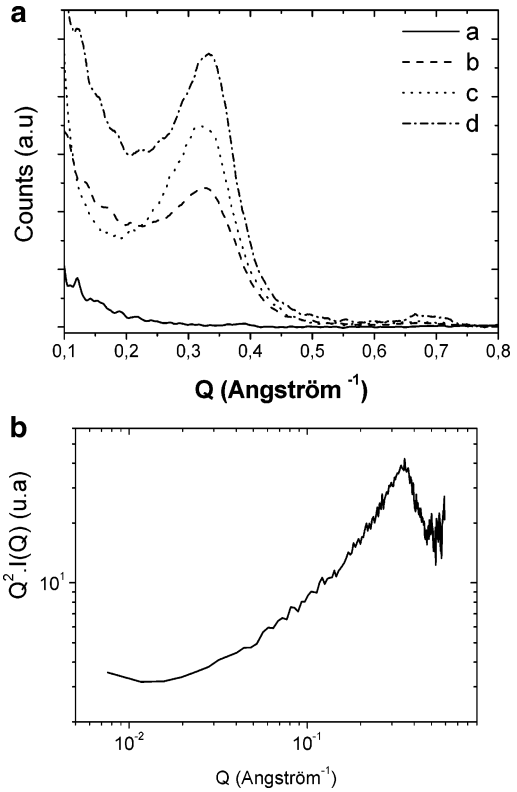

Figure 2. (a) X-ray diffraction patterns of PEO/laponite nanocomposites, with different concentrations (weight percent) on starved laponite particles. (a) PEO 10000 neat, (b) 3.75%, (c) 6.5% and (d) 10%. (b) Small angle X-ray spectrum of a 6.5% of starved laponite particles in PEO 10000.

data of starved laponite particles (with PEO 10000 adsorbed chains) are presented. Pure PEO shows essentially a power law behavior over all the frequency range for G'' that allows us to determine the viscosity of the polymer matrix. A Newtonian behavior is observed with $\eta_0 = 2.15$ Pa·s. G' for pure PEO can only be detected at the highest frequencies and shows an ω^2 dependence as expected.

As the concentration is increased, although both moduli increase over all the frequency range, the most remarkable feature is the strong increase in G' at low frequencies and the apparition of a plateau in both G' and G'' above a sufficiently high concentration (3.75 wt % under these conditions). This general behavior reflects a classical liquid−solid or liquid-gel transition for PLSN, already reported in the literature. The gelation concentration, on the basis of the Winter and Chambon criterion[17] appears for 1 wt % of starved particles, as shown in Figure 4, where G' and G'' show the same power law dependence with frequency ($G' \propto G'' \propto \omega^{\Delta}$) and where tan δ is thus independent of the frequency.

The large increase in viscosity at low frequency is better seen in Figure 5 where the complex viscosity (η^*) is plotted vs frequency. The similarity of the various curves has been used to obtain a master curve (Figure 6) using the reduced dimensionless variables η^*/η^*_{inf} as a function of $\omega\eta^*_{inf}/G'_0$ as proposed by Rodlert et al.[46] The limiting viscosity at high frequency (η^*_{inf}) is obtained by fitting the curves of Figure 6 and the complex plateau modulus is read directly for each concentration (Figures 3). The existence of a master curve shows that the behavior of the complex viscosity is identical for all the concentrations in particles, provide that the frequency is rescaled by a characteristic relaxation time $\lambda_c = \eta^*_{inf}/G_0^*$ and the viscosity is normalized by the high-frequency limiting

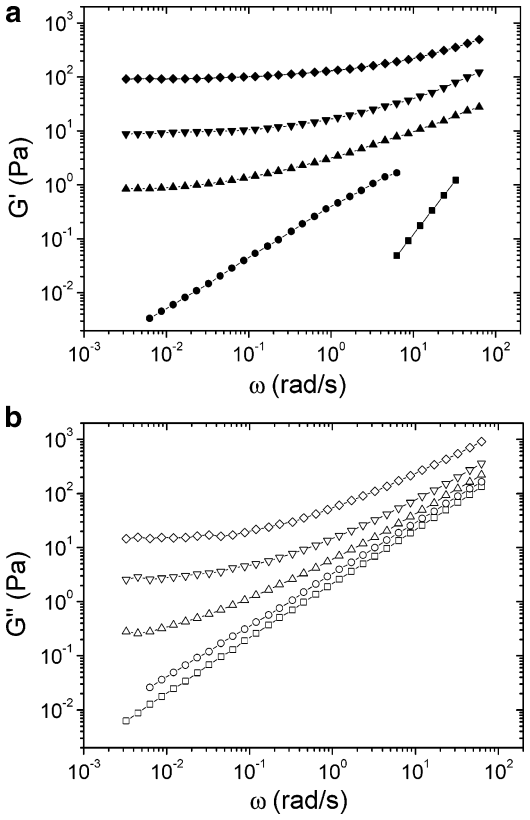

Figure 3. (a) Storage modulus G' and (b) Loss modulus G'' vs frequency ω at 80°C, for several different starved laponite particles loadings (weight percent). PEO 10000 neat (■□), 1% (●○), 3.75% (▲△), 6.5% (▼▽) and 10% (◆◇).

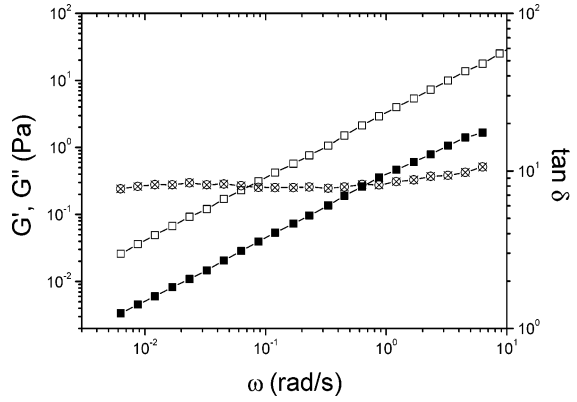

Figure 4. Evolution of rheological parameters vs frequency ω for nanocomposites with 1 wt % of starved laponite particles at 80°C. G' (■), G'' (□) and tan δ (⊗).

viscosity. This characteristic time decreases with the concentration of laponite ($\lambda_c \approx \phi^{-3.4}$ as shown in the inset of Figure 6) and essentially defines the point at which the viscoelastic behavior deviates from that of the matrix. The high-frequency range is dominated by the dynamics of the matrix and values close to those of the matrix show that the effect of the particles is small. The high-frequency limiting viscosity increases with the concentration of particles according to a Quemada law $\eta_{inf} = \eta_0(1 - \phi/\phi_m)^{-2}$ with $\phi_m = 17\%$ (by weight).

Since flow curves of the same samples were available, the steady state viscosity vs shear rate and the complex viscosity vs frequency were plotted together on Figure 7. Very clearly, the Cox−Merz rule does not apply for these materials and the viscosity under flow is always below the complex viscosity, in agreement with a destruction of the organization of the particles

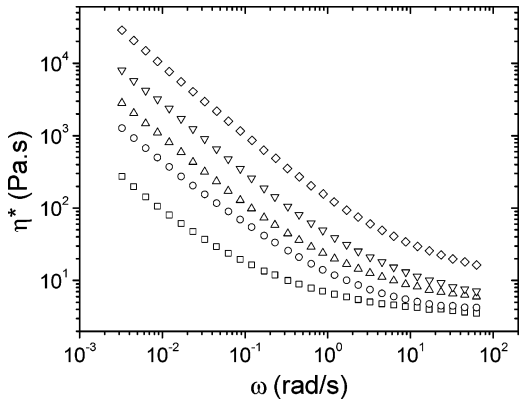

Figure 5. Dynamic complex viscosity η^* vs frequency ω at 80 °C. 3.75% (□), 5% (○), 6.5% (△), 7.5% (▽), and 10% (◇) (starved particles).

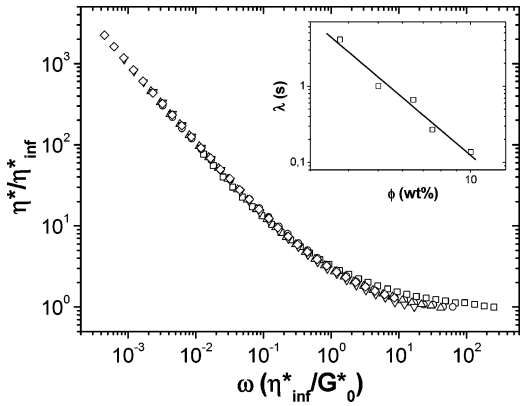

Figure 6. Dimensionless diagram η^*/η_{inf}^* as a function of $\omega \cdot \eta_{inf}^*/G_0'$. representing master-curve obtained from the complex viscosity of nanocomposites at several clay loadings: 3.75% (□), 5% (○), 6.5% (△), 7.5% (▽), and 10% (◇) (starved particles). The characteristic time $\lambda = \eta_{inf}^*/G_0'$ is shown in the inset vs the clay weight fraction.

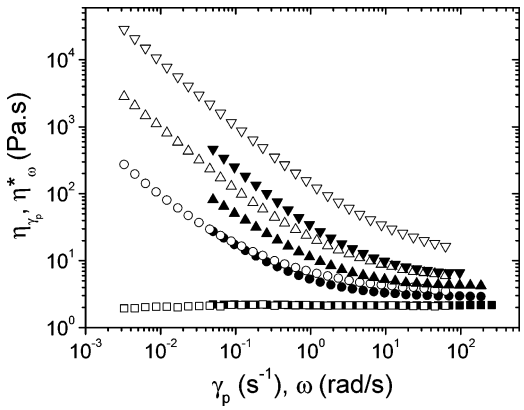

Figure 7. Cox−Merz representation of nanocomposites based on starved particles: open symbols, dynamic data; closed symbols, steady-state flow data.

under flow. The higher the concentration in particles, the more pronounced the effect. The nonvalidity of the Cox−Merz rule has been noted previously[12] in PLSN.

Influence of the Protection of the Particles. As mentioned in the Introduction, the protection of the particles and hence the compatibility with the matrix can be varied from bare particles, which show only a small affinity with the matrix chains to particles grafted at saturation with PEO chains, which are expected to show the greatest affinity with the matrix. Intermediate states consist of particles bearing adsorbed chains either with a full or only partial coverage. Although the molecular

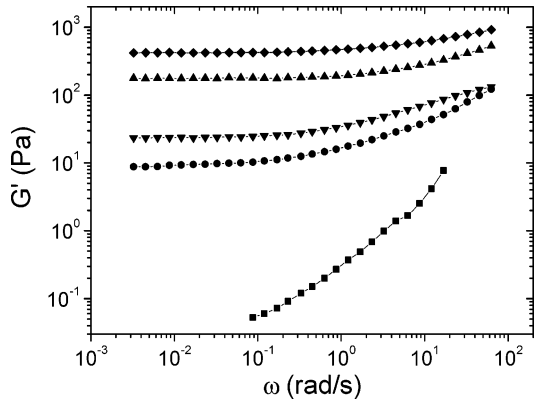

Figure 8. Storage modulus as a function of frequency for nanocomposites PEO/laponite, with different treatments of laponite particles at 6.5 wt %: (■) bared; (●) starved adsorbed; (▲) starved grafted; (▼) saturated adsorbed; (◆) saturated grafted.

weight of the grafted chains is much smaller than that of the adsorbed chains, the comparison of both types of protection is relevant since the equilibrium surface coverage is about the same.

We first investigated the effect of surface coverage by chain's adsorption onto the particles on the viscoelastic properties. In Figure 8, we compare nanocomposites at the same particles concentration 6.5 wt %. Incorporated particles are either bared (but the dispersion in water followed by the freeze-drying process has been carried out), starved (adsorption 1/1) or saturated (adsorption 2.5/1). The molecular weight of the adsorbed chains is the same as that of the matrix. Under these conditions, the possible exchange between absorbed species and free species is quite small, since it does not bring any entropic gain.

A slight reinforcing effect as compared to pure PEO can be seen with the bare particles, but the increase in the moduli is more important when particles are protected with PEO chains before compounding. The highest effect is seen with saturated particles.

Second, we compared particles fully covered with adsorbed or grafted chains. Although both types of particles bear the same surface coverage, the highest moduli, i.e., the highest reinforcing effect is observed with the grafted chains. This effect is however weaker (difference of about a factor of 2) than the influence of the surface coverage (a factor larger than 10).

It thus clearly appears that the type of protection of the particles plays an important role on the rheological properties of the materials. A possible explanation lies on the dispersion of the particles, since the rheological behavior of suspensions depends on the effective volume fraction of particles and also on their ability to form large scale open aggregates.

The state of dispersion of the particles can be compared, at least qualitatively, using X-ray data, which are plotted in Figure 9 for a particle concentration of 6.5%. The intensity of the Bragg peak clearly decreases when going from bared, to starved and saturated particles with adsorbed chains. As grafted chains are considered, the Bragg peak has almost disappeared which tends to prove that the particles are well separated or at least do not exist as stacks as in the other cases. One might notice that, taking into account the investigated q range (0.1−1 Å^{-1}), long-range correlations at distances smaller than 3−4 nm are excluded. Since no correlation peak was seen in SAXS for the 6.5 wt % sample with starved particles (see Figure 2b), the existence of long-range correlations with saturated particles is unlikely.

The decrease of the Bragg peak goes together with an increase of the reinforcing effect. This shows that the elastic moduli are

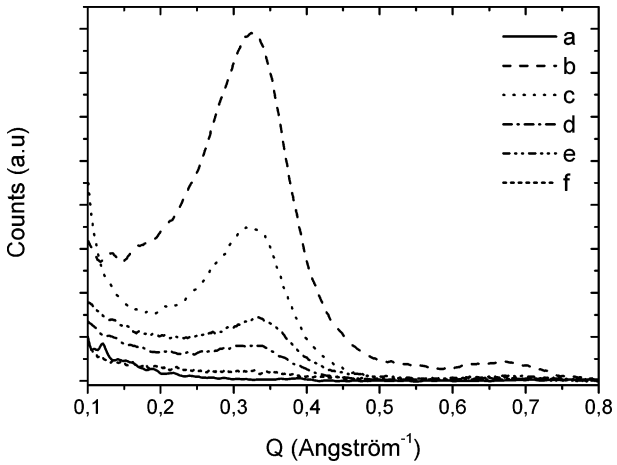

Figure 9. X-ray diffraction patterns of nanocomposites PEO/laponite, with different treatments of laponite particles at 6.5 wt %: (a) PEO 10000 neat; (b) bare; (c) starved adsorbed; (d) saturated adsorbed; (e) starved grafted; (f) saturated grafted.

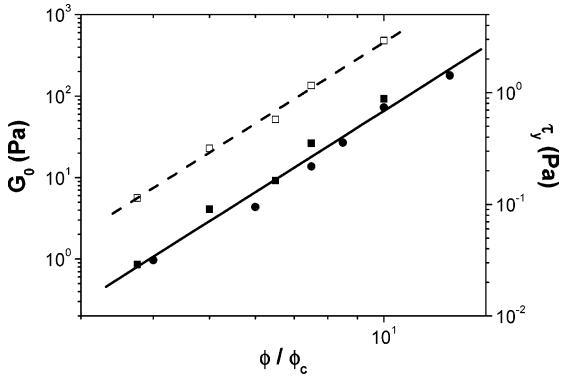

Figure 10. Scaling law of G_0 (closed symbols) and τ_y (open symbols) vs the reduced volume fraction: squares: starved particles; circles: saturated particles.

directly related to the fraction of correctly (i.e., not as compact aggregates) dispersed particles, for a given matrix.

This idea is substantiated by the change in the percolation threshold as the protection of the particles is varied. Indeed, percolation is observed at 1% for starved (adsorption 1/1) particles, whereas it is noted at only 0.5% with saturated particles (adsorption 2.5/1), in agreement with an improved state of dispersion.

Scaling Laws for the Elastic Modulus and the Yield Stress. In the gel state (above the percolation threshold), the nanocomposites show an equilibrium elastic modulus and a yield stress which both increase strongly with the fraction of particles and more precisely with the volume fraction of dispersed particles, since it also depends on the dispersion state at a given volume fraction of particles. The elastic modulus is plotted vs the reduced quantity ϕ/ϕ_c (where ϕ is the weight fraction of particles and ϕ_c the weight fraction at the percolation threshold) in Figure 10. It can be seen, that whatever the type of particle's protection, the following scaling law applies: $G_0 \propto (\phi/\phi_c)^{4.5\pm0.2}$

The value of the exponent does not depend on the type of protection, taking into account the various experimental uncertainties. Moreover, the quantitative superposition of moduli obtained using saturated and starved particles when plotted vs ϕ/ϕ_c shows that the same structure is at the origin of the viscoelastic properties in both types of nanocomposites. This observation reinforces the idea that the moduli are related to the fraction of exfoliated particles that are able to reorganize into a fractal structure as discussed below.

The yield stress has also been evaluated for starved particles bearing adsorbed chains and the scaling behavior is plotted in Figure 10. The yield stress scales as $\tau_y \propto (\phi/\phi_c)^{3.3\pm0.2}$.

Scaling relationships between elastic modulus or yield stress and concentration or volume fraction of dispersed species have been reported in various systems like colloïdal silica in poly(dimethylsiloxane),[47] polyols,[48,49] and polybutadiene.[50] They are expected theoretically[51,52] but to our knowledge, no scaling has been reported for lamellar particles dispersed in polymeric matrices.

Discussion

In this discussion we would like to emphasize the main tendencies observed upon incorporation of laponite particles into a PEO matrix and to compare them with other systems where the filler consists either of lamellar particles or of spherical ones. We would like to point out mainly two aspects: the fractal nature of the gel and the relationship between the elastic modulus of the gel and the state of dispersion of the particles.

With this model system, the general effect upon incorporating laponite particles into a PEO matrix is, from a rheological point of view, to transform the resulting material from a viscoelastic liquid into a viscoelastic solid. The solidlike character is observed above a given concentration, called here percolation concentration, since at this particular concentration, the dynamic moduli scale with the same power of the frequency, as it is usually observed in gelation processes.[17] It is however not totally proved that this change of behavior fully follows the expectations of a percolation process. Indeed, the expected value for percolation is close to 0.7,[53] whereas our data lead to a relaxation exponent of 0.93. However, it is known that the relaxation exponent is very sensitive to experimental conditions.

To our knowledge, the existence of a critical concentration of particles in layered silicates nanocomposites has not been reported, contrary to carbon nanotubes polymer nanocomposites.[16,54] The percolation threshold appears to be very low in laponite−PEO systems (on the order of 1 wt %, or equivalently for occupied volume fractions as low as 0.4%). It is also highly dependent on the type of protection of the particles. It has been shown to decrease from 1 wt % when the surface of the particles is not fully covered down to 0.5% with saturated particles. This observation, substantiated with the X-ray data that suggest a better dispersion of the particles as individual objects when the particles are totally protected, shows that the percolation concentration is directly related to the dispersion of the nanoparticles as individual objects. It suggests that the gel is obtained through physical contacts or at least strong interactions between essentially isolated particles and that the gel strength is linked to the number of connected strands of particles, like in polymer networks.

According to Ren et al.,[11] the weight fraction of particles at percolation can be calculated on the basis of percolating spheres, each sphere containing a given number of stacked particles. If a full dispersion of the particles can be obtained, only one particle is contained into a sphere of 30 nm diameter. The volume fraction at the percolation concentration of randomly distributed spheres (0.3) is related to the weight fraction w_L of laponite particles by

$$\phi_{per} = \frac{4R}{3h}\left[\frac{w_L\rho_p}{(1-w_L)\rho_L + w_L\rho_p}\right]$$

where h and R are respectively the thickness and the radius of a laponite particle and ρ_L and ρ_p the densities of laponite and polymer, respectively.

This expression can be simplified when $w_L \ll 1$ into

$$w_L \cong \frac{3\phi_{per}h}{4R}\frac{\rho_L}{\rho_p}$$

Applying this relation to the laponite/PEO system yields a percolation concentration of laponite of 3.75 wt %. This concentration is much larger than the percolation transition observed at 0.5 or 1 wt % depending on the protection of the particles. Therefore, the random distribution of isolated particles interacting through excluded volume interactions is probably not valid in this system. Rather, association of laponite particles into a fractal structure seems more compatible with the very low concentration observed at percolation. Such a behavior has already been observed with laponite suspensions in water, even in the presence of low concentration of PEO chains.[42]

According to a modeling of the modulus and the yield stress of suspensions of aggregates with a fractal dimension D,[51] both quantities scale with a power of the volume fraction of particles as $G_0 \approx \phi^{5/(3-D)}$ and $\tau_y \approx \phi^{4/(3-D)}$. Both scaling laws were shown to apply in Silica-Silicone suspensions.[49,51] Other scaling relationships are available,[52] but they involve the fractal dimension of the backbone which is unknown. In our laponite−PEO system, Figure 10 shows that the scaling laws apply and the fractal dimension coming out from the equilibrium modulus or the yield stress is 1.9 and 1.8, respectively. These values are very close to those reported on silica dispersions,[49] but the percolation threshold seems much lower in our case (less than 0.5% in volume against 2% with spherical silica).

One might note that this fractal dimension is very close, although somewhat lower, to that of aggregates of laponite particles in water where $D = 2$.

The zero shear modulus in laponite−PEO suspensions can be compared to that of laponite suspensions in water which also lead to fragile gels. The following relationship has been shown to hold:[55] $G'(\text{Pa}) = 18C^{3.5}$ when the concentration is expressed in weight %. In this case, electrostatic attraction between positively charged edges and negatively charged faces is responsible for the aggregation of the particles although no short range order exists as in the house of cards picture.[56] In PEO, the order of magnitude of the moduli is 200 Pa for 10 wt % laponite against 57000 Pa for laponite in water assuming that the scaling law holds at such high concentrations. Although different kinds of interactions are at the origin of aggregation in both types of systems, the repulsion between particles must be much lower in the polymer matrix where long-range repulsive interactions are not expected.

The value of the equilibrium moduli (200 Pa for a volume fraction of 2.5%) is quite comparable to that measured with hydrophobic silica in a low molecular weight polyol,[49] with a viscosity of the matrix that is by a factor of 4 lower than in our case.

The second point we would like to emphasize is related to the limiting elastic modulus of the suspensions above percolation. It has been clearly shown that, for a given system (i.e., laponite in PEO matrix), the level of the elastic modulus increases not only with concentration, but also changes depending on the type of protection and thus on the dispersion of the particles, as demonstrated by X-ray scattering data. The increase in the modulus is strongly linked, at a given concentration, to the dispersion of the particles as individual objects. It can thus be concluded that, above percolation, the zero shear modulus

essentially reflects the fraction of well dispersed objects (that are not observed in X-ray data) and that poorly dispersed domains essentially do not contribute to the modulus, since they do not contribute to the number of connected species. The determination of the prefactor of the scaling law is still unknown, but is clearly related to the strength of the interactions between the particles that form the aggregates. According to the model of Piau et al.,[51] the prefactor is linked both to the free energy level of a reference volume and to the percolation concentration. In an other view[52] of the elasticity of fractal objects, the prefactor is related to the spring constant of the fractal object, which involves unbending of the strings with deformation.

Conclusions

In this study, model nanocomposites based on laponite particles and PEO where obtained through a specific protection of the laponite particles against aggregation together with the introduction of organic polymer chains onto their surface through PEO adsorption or cationic exchange of end-terminated trimethylammonium−PEO chains. The protected particles were isolated from the adsorption medium with a freeze-drying procedure and were mixed into the PEO matrix in the molten state using a micromixer. The state of dispersion depends on the surface coverage of the particles and essentially complete exfoliation is observed with saturated particles bearing grafted chains rather than adsorbed ones.

The viscoelastic properties show a transition from a viscoelastic liquid to a viscoelastic solid behavior above a critical concentration where a relaxation exponent can be determined. This critical concentration (0.5 wt % or 0.2% volume fraction) is much below the percolation transition of spheres based on the dimensions of the platelets which would interact through excluded volume. This critical concentration also decreases when the particles are better dispersed which is coherent with the formation of a gel through a network of interacting particles.

The elastic modulus of the gels as well as the yield stress show a power law behavior with the volume fraction of particles, as observed in various suspensions of aggregated particles. The fractal dimension of the particle network is equal to 1.9, i.e., is slightly below that observed with laponite particles in water.

Acknowledgment. This work was financially supported by the French Ministry for National Education and Research (MENESR) and the "Région des Pays de la Loire" under the Program of the "Contrat Etat Région no. 18026 Polymères-Plasturgie". Their support is acknowledged with gratitude. The help of Prof. A. Gibaud and Dr. Jean-François Bardeau with the X-ray measurements is gratefully acknowledged.

References and Notes

(1) Alexandre, M.; Dubois, P. *Mater. Sci. Eng.: R, Rep.* **2000**, *28*, 1−63.
(2) Ellis, T. S. *Polymer* **2003**, *44*, 6443−6448.
(3) Vaia, R. A.; Ishii, H.; Giannelis, E. P. *Chem. Mater.* **1993**, *5*, 1694−1696.
(4) Giannelis, E. P.; Krishnamoorti, R.; Manias, E. *Adv. Polym. Sci.* **1999**, *138*, 107−147.
(5) Gopakumar, T. G.; Lee, J. A.; Kontopoulou, M.; Parent, J. S. *Polymer* **2002**, *43*, 5483−5491.
(6) Chrissopoulou, K.; Altintzi, I.; Anastasiadis, S. H.; Giannelis, E. P.; Pitsikalis, M.; Hadjichristidis, N.; Theophilou, N. *Polymer* **2005**, *46*, 12440−12451.
(7) Krishnamoorti, R.; Vaia, R. A.; Giannelis, P. *Chem. Mater.* **1996**, *8*, 1728−1734.
(8) Jeon, H. S.; Rameshwaran, J. K.; Kim, G.; Weinkauf, D. H. *Polymer* **2003**, *44*, 5749−5758.
(9) Hyun, Y. H.; Lim, S. T.; Choi, H. J.; Jhon, M. S. *Macromolecules* **2001**, *34*, 8084−8093.
(10) Krishnamoorti, R.; Yurekli, K. *Curr. Opin. Colloid Interface Sci.* **2001**, *6*, 464−470.
(11) Ren, J. X.; Silva, A. S.; Krishnamoorti, R. *Macromolecules* **2000**, *33*, 3739−3746.
(12) Ren, J.; Krishnamoorti, R. *Macromolecules* **2003**, *36*, 4443−4451.
(13) Solommon, M. J.; Almusallam, A. S.; Sefeldt, K. F.; Somwangthanaroj, A.; Varadan, P. *Macromolecules* **2001**, *34*, 1864−1872.
(14) Moussaif, N.; Groeninckx, G. *Polymer* **2003**, *44*, 7899−7906.
(15) Galgali, G.; Ramesh, C.; Lele, A. *Macromolecules* **2001**, *34*, 852−858.
(16) Kelarakis, A.; Yoon, K.; Somani, R. H.; Chen, X.; Hsiao, B. S.; Chu, B. *Polymer* **2005**, *46*, 11591−11599.
(17) Winter, H. H.; Chambon, F. *J. Rheol.* **1986**, *30*, 367−382.
(18) Chambon, F.; Winter, H. H. *J. Rheol.* **1987**, *31*, 683−697.
(19) Zhang, Q.; Archer, L. A. *Langmuir* **2002**, *18*, 10435−10442.
(20) Vermogen, A.; Masenelli-Varlot, K.; Séguéla, R.; Duchet-Rumeau, J.; Boucard, S.; Prele, P. *Macromolecules* **2005**, *38*, 9661−9669.
(21) Kroon, M.; Vos, W. L.; Wegdam, G. H. *Phys. Rev. E* **1998**, *57*, 1962−1970.
(22) Laporte_Industrie_Ltd. *Laponite Technical Bulletin*, Cheshire, UK, 1990; *L104/90/A*, 1−15.
(23) Doeff, M. M.; Reed, J. S. *Solid State Ionics* **1998**, *113−115*, 109−115.
(24) Chen, W.; Xu, Q.; Yuan, R. Z. *Mater. Sci. Eng. B* **2000**, *77*, 15−18.
(25) Aranda, P.; Ruiz-Hitzky, E. *Chem. Mater.* **1992**, *4*, 1395−1403.
(26) Chen, H.-W.; Chang, F.-C. *Polymer* **2001**, *42*, 9763−9769.
(27) Loyens, W.; Jannasch, P.; Maurer, F. H. J. *Polymer* **2005**, *46*, 903−914.
(28) Shen, Z.; Simon, G. P.; Cheng, Y.-B. *Polymer* **2002**, *43*, 4251−4260.
(29) Shen, Z.; Simon, G. P.; Cheng, Y.-B. *Polym. Eng. Sci.* **2002**, *42*, 2369−2383.
(30) Loyens, W.; Jannasch, P.; Maurer, F. H. J. *Polymer* **2005**, *46*, 915−928.
(31) Gournis, D.; Floudas, G. *Chem. Mater.* **2004**, *16*, 1686−1692.
(32) Baghdadi, H. A.; Sardinha, H.; Bhatia, S. R. *J. Polym. Sci. Part B: Polym. Phys.* **2005**, *43*, 233−240.
(33) Dundigalla, A.; Lin-Gibson, S.; Ferreiro, V.; Malwitz, M. M.; Schmidt, G. *Macromol. Rapid Commun.* **2005**, *26*, 143−149.
(34) Loizou, L.; Butler, P. D.; Porcar, L.; Kesselman, E.; Talmon, Y.; Dundigalla, A.; Schmidt, G. *Macromolecules* **2005**, *38*, 2047−2049.
(35) Loizou, E.; Butler, P.; Porcar, L.; Schmidt, G. *Macromolecules* **2006**, *39*, 1614−1619.
(36) Malwitz, M. M.; Butler, P. D.; Porcar, L.; Angelette, D. P.; Schmidt, G. *J. Polym. Sci., Part B−Polym. Phys.* **2004**, *42*, 3102−3112.
(37) Schmidt, G.; Nakatani, A. I.; Butler, P. D.; Karim, A.; Han, C. C. *Macromolecules* **2000**, *33*, 7219−7222.
(38) Morvan, M.; Espinat, D.; Lambard, J.; Zemb, T. *Colloids Surf. A-Physicochem. Eng. Asp.* **1994**, *82*, 193−203.
(39) Tawari, S. L.; Koch, D. L.; Cohen, C. *J. Colloid Interface Sci.* **2001**, *240*, 54−66.
(40) Nicolai, T.; Cocard, S. *Eur. Phys. J. E* **2001**, *5*, 221−227.
(41) Nicolai, T.; Cocard, S. *J. Colloid Interface Sci.* **2001**, *244*, 51−57.
(42) Mongondry, P.; Nicolai, T.; Tassin, J.-F. *J. Colloid Interface Sci.* **2004**, *275*, 191−196.
(43) Nelson, A.; Cosgrove, T. *Langmuir* **2004**, *20*, 10382−10388.
(44) Mongondry, P.; Bonnans-Plaisance, C.; Jean, M.; Tassin, J. F. *Macromol. Rapid Commun.* **2003**, *24*, 681−685.
(45) Loyens, W.; Maurer, F. H. J.; Jannasch, P. *Polymer* **2005**, *46*, 7334−7345.
(46) Rodlert, M.; Plummer, C. J. G.; Leterrier, Y.; Manson, J.-A. E.; Grunbauer, H. J. M. *J. Rheol.* **2004**, *48*, 1049−1065.
(47) Aranguren, M. I.; Mora, E.; De Groot, J. V.; Macosko, C. W. *J. Rheol.* **1992**, *36*, 1165−1182.
(48) Khan, S. A.; Zoeller, N. J. *J. Rheol.* **1993**, *37*, 1125−1235.
(49) Saint-Michel, F.; Pignon, F.; Magnin, A. *J. Colloid Interface Sci.* **2003**, *267*, 314−319.
(50) Zhu, Z.; Thompson, T.; Wang, S.-Q.; von Meerwall, E. D.; Halasa, A. *Macromolecules* **2005**, *38*, 8816−8824.
(51) Piau, J. M.; Dorget, M.; Palierne, J. F.; Pouchelon, A. *J. Rheol.* **1999**, *43*, 305−314.
(52) Shih, W.-H.; Shih, W. Y.; Kim, S.-I.; Aksay, I. A. *Phys. Rev. A* **1990**, *42*, 4772−4779.
(53) Winter, H. H.; Mours, M. *Adv. Polym. Sci.* **1997**, *134*, 165.
(54) Liu, Z.; Chen, K.; Yan, D. *Eur. Polym. J.* **2003**, *39*, 2359−2366.
(55) Cocard, S.; Université du Maine: Le Mans, France, 1999; p 258.
(56) Mongondry, P.; Tassin, J. F.; Nicolai, T. *J. Colloid Interface Sci.* **2005**, *283*, 397−405.
(57) *Physical Properties of Polymer Handbook*; Mark, James E., Ed.; AIP Press: Woodbury, NY, 1996.

MA061324W